AIP Applied Physics Letters

Effect of dislocations on local transconductance in AlGaN/GaN heterostructures as imaged by scanning gate microscopy

J. W. P. Hsu, N. G. Weimann, M. J. Manfra, K. W. West, D. V. Lang et al.

Citation: Appl. Phys. Lett. 83, 4559 (2003); doi: 10.1063/1.1629143
View online: http://dx.doi.org/10.1063/1.1629143
View Table of Contents: http://apl.aip.org/resource/1/APPLAB/v83/i22
Published by the American Institute of Physics.

Related Articles

Ultra-low resistance ohmic contacts in graphene field effect transistors
Appl. Phys. Lett. 100, 203512 (2012)

Three-dimensional distribution of Al in high-k metal gate: Impact on transistor voltage threshold
Appl. Phys. Lett. 100, 201909 (2012)

Electric field effect in graphite crystallites
Appl. Phys. Lett. 100, 203116 (2012)

Efficient terahertz generation by optical rectification in Si-LiNbO3-air-metal sandwich structure with variable air gap
Appl. Phys. Lett. 100, 201114 (2012)

Vertically integrated submicron amorphous-In2Ga2ZnO7 thin film transistor using a low temperature process
Appl. Phys. Lett. 100, 203510 (2012)

Additional information on Appl. Phys. Lett.

Journal Homepage: http://apl.aip.org/
Journal Information: http://apl.aip.org/about/about_the_journal
Top downloads: http://apl.aip.org/features/most_downloaded
Information for Authors: http://apl.aip.org/authors

ADVERTISEMENT

Downloaded 20 May 2012 to 128.210.126.199. Redistribution subject to AIP license or copyright; see http://apl.aip.org/about/rights_and_permissions

Effect of dislocations on local transconductance in AlGaN/GaN heterostructures as imaged by scanning gate microscopy

J. W. P. Hsu,[a] N. G. Weimann, M. J. Manfra, K. W. West, D. V. Lang, F. F. Schrey,[b] and O. Mitrofanov
Bell Laboratories, Lucent Technologies, Murray Hill, New Jersey 07974

R. J. Molnar
Lincoln Laboratory, Massachusetts Institute of Technology, Lexington, Massachusetts 02420-9108

(Received 1 May 2003; accepted 26 September 2003)

The spatial variations of transconductance in AlGaN/GaN heterostructures were mapped using a conducting tip atomic force microscope. The conducting tip locally modulates the two-dimensional electron gas (2DEG) while the change in the drain current was monitored as a function of tip position. A spatial resolution of 250 nm was obtained. This technique enables us to investigate the role of defects in transistor performance. In particular, when biased near the depletion of the 2DEG, the transconductance map displays a cell structure, with low signal regions correlating with the positions of negatively charged threading dislocations. *© 2003 American Institute of Physics.* [DOI: 10.1063/1.1629143]

AlGaN/GaN high electron mobility transistors (HEMTs) are promising candidates for high power, high frequency electronics. One important parameter of a transistor is the transconductance, the response in the drain current to a change in the gate voltage. Due to the lack of lattice-matched substrates, GaN films typically contain a high density of threading dislocations. In addition, alloy fluctuations can exist in the AlGaN barrier, and traps in the barrier and/or the substrate can cause degradation of device performance. Such defects and inhomogeneities will result in a spatially nonuniform transconductance. Here, we map the transconductance variation in AlGaN/GaN heterostructures using the conducting tip of an atomic force microscope (AFM) as the gate, i.e., scanning gate microscopy (SGM).[1] The SGM provides a direct way to evaluate the role of defects on the HEMT performance. Previously, SGM has been used for basic studies in physics.[2–4] This work demonstrates that SGM is also a powerful technique for device characterization.

The spatial variations in GaN electrical properties that are associated with dislocations have been studied using conducting tip AFM.[5–9] In SGM, the conducting tip acts as a nanometer-size gate that can be scanned over the region between the source and drain of a transistor. In the case of AlGaN/GaN HEMTs, the two-dimensional electron gas (2DEG) directly beneath the tip is modulated due to the field of the tip. In our setup (Fig. 1), in addition to the dc voltages applied between the drain and source (V_{ds}) and that between the gate and source (V_{gs}), a small ac bias (v_{ac}), typically, at 20 kHz, is applied to the tip (gate). The small-signal transconductance (g_m) is defined as $g_m = di_{ac}/dv_{ac}$, where i_{ac} is the ac component of the drain–source current at the frequency of v_{ac}, demodulated using a lock-in amplifier. In comparison to previous work,[1–4] adding v_{ac} to V_{gs} not only enhances the signal-to-noise ratio but also enables us to directly map the spatial variations in g_m.

The samples are GaN films with $Al_{0.3}Ga_{0.7}N$ barriers grown by molecular beam epitaxy on semi-insulating GaN templates prepared by hydride vapor phase epitaxy (HVPE).[10] HVPE templates serve as a quasibulk substrate with a relatively low threading dislocation density (10^8–10^9 cm^{-2}). Our AlGaN/GaN heterostructures, typically, exhibit a room temperature 2DEG density of 1.2×10^{13} cm^{-2} and a mobility of $\sim$1500 cm^2/V s, as determined by Hall measurements. To map the spatial variations in transconductance, transistor structures without metal gates are required. Furthermore, because of the small size of the AFM tip ($\leqslant$50 nm), the width of the channel needs to be small so that the response to the tip (gate) will be measurable. This is achieved by using a "bowtie" shaped mesa with a narrow region between the Ohmic source and drain contacts. The width at the neck of the bowtie is $\sim$3 μm and the length of the bowtie (distance between source and drain) is typically 5.5 μm. A three-dimensional rendering of the topography of such a gateless transistor is shown in Fig. 1. These gateless transistors are dispersed among regular metal-gate (Ni/Au) HEMTs so that the transconductance map ob-

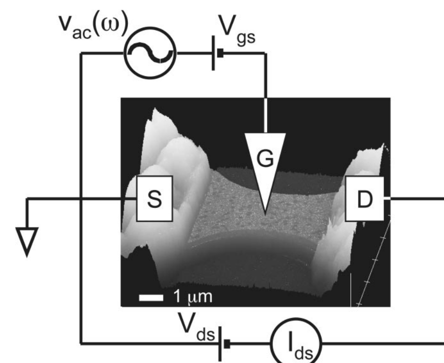

FIG. 1. Schematics of our SGM setup for mapping transconductance (g_m) variations. The picture is a three-dimensional rendering of an AFM topographic image of a gateless AlGaN/GaN HEMTs.

[a]Author to whom correspondence should be addressed; current address: Sandia National Laboratories, P.O. Box 5800, MS-1415, Albuquerque, NM 87185; electronic mail: jhsu@mailaps.org
[b]Current address: Technische Universität Wien, Floragasse 7,1040 Wien, Austria.

 © 2003 American Institute of Physics

Downloaded 20 May 2012 to 128.210.126.199. Redistribution subject to AIP license or copyright; see http://apl.aip.org/about/rights_and_permissions

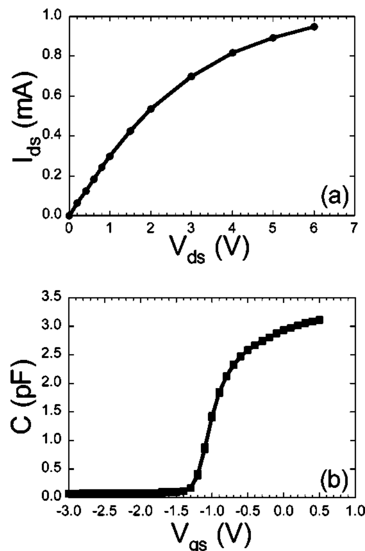

FIG. 2. (a) $I-V$ of a 3-μm-wide gateless AlGaN/GaN transistor. (b) $C-V$ of adjacent metal-gate HEMTs (gate length $=2$ μm and gate width $=200$ μm).

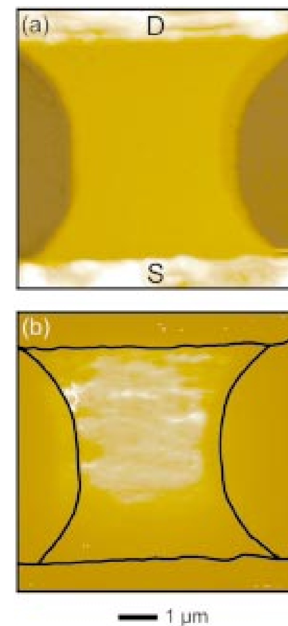

FIG. 3. (Color) 7 μm$\times$7 μm (a) topography and (b) transconductance images of a 3-μm-wide gateless transistor. S: source, held at ground potential; D: drain, positively biased. $V_{ds}=1$ V, $V_{gs}=0.5$ V, and $v_{ac}=0.1$ V_{rms}. The outlines of the mesa determined from the topographic image (a) are overlaid on the transconductance image (b). The gray scales represent 700 nm and 10^{-5} S in (a) and (b), respectively.

tained from the SGM experiment can be correlated with the performance of real devices.

The devices shown in this letter were fabricated on a wafer grown under stoichiometric conditions to minimize gate leakage.[5,11] This type of growth displays the characteristic topography of pits associated with the surface terminations of threading dislocations.[5,8] The device processing procedures used on this wafer caused some etching of the AlGaN barrier. Consequently, the thickness of the AlGaN barrier in the final devices was reduced from the nominal thickness of 25 nm to ~12 nm, as estimated from capacitance–voltage ($C-V$) measurements on metal-gate transistors. Moreover, the depths of the dislocation pits are amplified and the overall 2DEG density was reduced. Figure 2(a) shows a current–voltage ($I-V$) curve for a gateless HEMT used in the SGM experiment. Since AlGaN/GaN HEMTs are charge-controlled devices, the $C-V$ characteristic is important for understanding the charge modulation behavior in the 2DEG channel. Figure 2(b) shows $C-V_{gs}$ for metal-gate HEMTs on the same chip as the gateless bow-tie transistors shown in Figs. 2(a), 3, and 4. The 2DEG is depleted at a gate bias of -1.0 to -1.5 V due to the lower 2DEG density of this particular sample. Even though the inadvertent etching of the AlGaN barrier degrades the HEMT performance, the demonstration of the SGM technique is not impacted.

Figure 3 shows simultaneously acquired (a) topographic and (b) g_m ($V_{ds}=1$ V and $V_{gs}=+0.5$ V) images of a gateless transistor. The outline of the mesa determined from the topographic image (a) is overlaid on the g_m image (b). As expected, the g_m signal is nonzero only where there is a 2DEG: the etched-away areas surrounding the mesa have no 2DEG, and the drain current cannot be modulated when the tip is over the Ohmic contacts. The ~0.4 μm shift between the two images is caused by the downward tilting of the cantilever, which extends to the right of the images, so that the end of the tip is closer to (farther away from) the side of the mesa when the tip is over the left (right) edge of the mesa, resulting in higher (lower) electric field. We observed that the g_m signal is very small near the source (ground), as seen in Fig. 3(b). This contrast increases as V_{ds} increases and is under further investigation. For the values of V_{ds} and V_{gs} used in the SGM experiments, the gate current in the metal-gate HEMT is at least four orders of magnitude smaller than the drain current. Attempts to image the gate leakage on the bowtie transistors using conducting tip AFM[5] show no measurable leakage under typical SGM conditions.

To better correlate the transconductance variations with defects, we performed high-resolution SGM measurements. Figure 4 shows simultaneously acquired (a) topographic and (b) g_m images taken at $V_{ds}=1$ V and $V_{gs}=-1$ V in a 2.5 μm$\times$2.5 μm area. The transistor in Fig. 4 is different from the one in Fig. 3, but they are on the same chip. At a gate bias of -1 V, the 2DEG is nearly depleted [Fig. 2(b)]. The g_m image shows a cell-like structure, with low g_m regions surrounded by high g_m boundaries. The low g_m regions *generally* correlate with the locations of topographic pits. The white lines in Fig. 4(b) are the perimeters of the pits in Fig. 4(a). Since there are no large topographic changes in these images, the position mismatch between topographic and g_m images that occurs at the mesa edges in Fig. 3 is not present. Figure 4(b) shows that the modulation of the 2DEG is less efficient when the tip (gate) is on top of the pits.

As mentioned previously, under stoichiometric growth conditions, pits are found at the surface terminations of threading dislocations.[5,8] Dislocations in GaN are negatively charged,[12] leading to a local depletion of the 2DEG.[13] The potential variations due to the excess fixed negative charge associated with the dislocations have been imaged by scanning Kelvin force microscopy (SKFM).[8,9] Figure 4(c) shows a surface potential map at the same sample positions as Figs. 4(a) and 4(b) taken with SKFM. By comparing Figs. 4(a) and 4(c), it is clear that negative charges [dark spots in Fig.

Downloaded 20 May 2012 to 128.210.126.199. Redistribution subject to AIP license or copyright; see http://apl.aip.org/about/rights_and_permissions

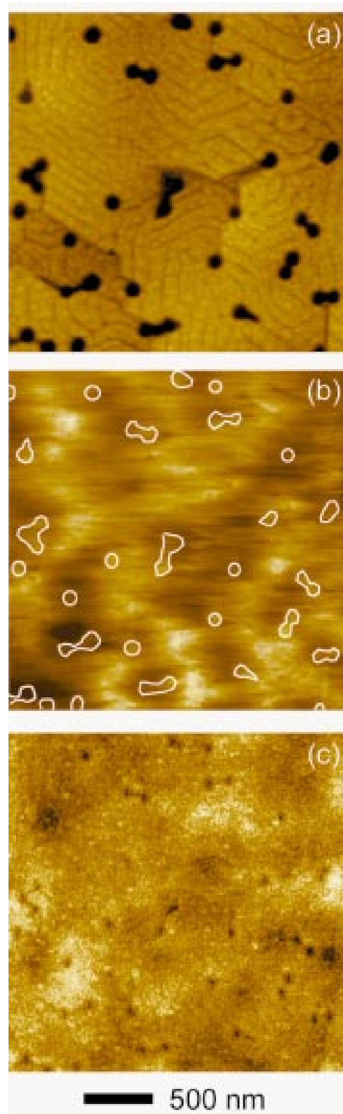

FIG. 4. (Color) 2.5 μm$\times$2.5 μm (a) topography and (b) transconductance images taken simultaneously. $V_{ds}=1$ V, $V_{gs}=-1$ V, and $v_{ac}=0.1$ V_{rms}. Lower transconductance signals appear dark in (b). The white lines in (b) outline the topographic pits in (a). (c) Surface potential map taken by scanning Kelvin force microscopy at the same sample positions as (a) and (b). Dark region in (c) corresponds to excess negative charge. The gray scales represent 30 nm, 2×10^{-5} S, and 0.2 V in (a), (b), and (c), respectively.

4(c)] are found at topographic pits. Threading dislocations are the most likely origins of these negative charges since transmission electron microscopy images show that threading dislocations are at the bottom of surface pits in this type of samples.[11] However, we cannot conclusively rule out non-(0001) planes or off-stoichiometric material in the defect pits as the source of the negative charge. In any case, the excess negative charge associated with a defect pit causes the depletion of the 2DEG in the surrounding region, which in turn results in lower transconductance locally.

Similar to scanning capacitance microscopy, the observed feature size in SGM is a convolution of the actual depletion region size, the physical size of the tip, and the barrier thickness.[7] To estimate the size of depletion region induced by the tip, we compare the measured SGM g_m value to that of metal-gate HEMTs on the same sample. Since we are in the linear $I_{ds}-V_{ds}$ regime, g_m is proportional to w/L, where w is the gate width and L is the gate length. The region gated by the tip will be a^2. At $V_{ds}=1$ V and $V_{gs}=-0.3$ V, the g_m of a 2 μm length$\times$25 μm width metal-gate HEMT is $\sim 8.75\times10^{-4}$ S. Hence, for a HEMT with $w=a$ and $L=a$, g_m would be 7×10^{-5} S. However, in the SGM experiment, only a fraction of the 2DEG is gated by the tip while current away from the tip flows unaffectedly. The ratio of the measured SGM g_m value (6×10^{-6} S) to 7×10^{-5} S is equal to a divided 3 μm. Thus, a is estimated to be $\sim$250 nm. This value agrees well with the size of the low g_m regions in the high-resolution SGM image [e.g., Fig. 4(b)].

In summary, we have shown that SGM is a powerful technique for mapping the electrical response of transistors with 250 nm resolution. For bias conditions near depletion, the transconductance map shows low signal regions correlate with the presence of threading dislocations, consistent with a lower 2DEG density in the vicinity of negatively charged dislocations.

The authors acknowledge R. De Picciotto, N. Zhitenev, and D. Monroe for useful discussions. The Lincoln Laboratory portion of this work was sponsored by the ONR under Air Force Contract No. F19628-00-C-0002.

[1] M. A. Eriksson, R. G. Beck, M. Topinka, J. A. Katine, R. M. Westervelt, K. L. Campman, and A. C. Gossard, Appl. Phys. Lett. **69**, 671 (1996).
[2] M. A. Topinka, B. J. LeRoy, S. E. J. Shaw, E. J. Heller, R. M. Westervelt, K. D. Maranowski, and A. C. Gossard, Science **289**, 2323 (2000); M. A. Topinka, B. J. LeRoy, R. M. Westervelt, S. E. J. Shaw, R. Fleischmann, E. J. Heller, K. D. Maranowski, and A. C. Gossard, Nature (London) **410**, 183 (2001).
[3] A. Bachtold, M. S. Fuhrer, S. Plyasunov, M. Forero, E. H. Anderson, A. Zettl, and P. L. McEuen, Phys. Rev. Lett. **84**, 6082 (2000).
[4] M. Freitag, M. Radosavljevic, Y. Zhou, A. T. Johnson, and W. F. Smith, Appl. Phys. Lett. **79**, 3326 (2001).
[5] J. W. P. Hsu, M. J. Manfra, D. V. Lang, S. Richter, S. N. G. Chu, A. M. Sergent, R. N. Kleiman, L. N. Pfeiffer, and R. J. Molnar, Appl. Phys. Lett. **78**, 1685 (2001).
[6] P. J. Hansen, Y. E. Strausser, A. N. Erickson, e. J. Tarsa, P. Kozodoy, E. G. Brazel, J. P. Ibbetson, U. Mishra, V. Narayanamurti, S. P. DenBaaars, and J. S. Speck, Appl. Phys. Lett. **72**, 2247 (1998).
[7] D. M. Schaadt, E. J. Miller, E. T. Yu, and J. M. Redwing, Appl. Phys. Lett. **78**, 88 (2001).
[8] J. W. P. Hsu, M. J. Manfra, D. V. Lang, K. W. Balwin, L. N. Pfeiffer, and R. J. Molnar, J. Electron. Mater. **30**, 110 (2001).
[9] G. Koley and M. G. Spencer, Appl. Phys. Lett. **78**, 2873 (2001); B. S. Simpkins, D. M. Schaadt, E. T. Yu, and R. J. Molnar, J. Appl. Phys. **91**, 9924 (2002).
[10] M. J. Manfra, N. G. Weimann, J. W. P. Hsu, L. N. Pfeiffer, K. W. West, S. Syed, H. L. Stormer, W. Pan, D. V. Lang, S. N. G. Chu, G. Kowach, A. M. Sergent, J. Caissie, K. M. Molvar, L. J. Mahoney, and R. J. Molnar, J. Appl. Phys. **92**, 338 (2002).
[11] J. W. P. Hsu, M. J. Manfra, S. N. G. Chu, C. H. Chen, and L. N. Pfeiffer, Appl. Phys. Lett. **78**, 3980 (2001).
[12] N. G. Weimann, L. F. Eastman, D. Doppalapudi, H. M. Ng, and T. D. Moustakas, J. Appl. Phys. **83**, 3656 (1998); D. Cherns and C. G. Jiao, Phys. Rev. Lett. **87**, 205504 (2001).
[13] K. V. Smith, E. T. Yu, J. M. Redwing, and K. S. Boutros, J. Electron. Mater. **29**, 274 (1999).

Downloaded 20 May 2012 to 128.210.126.199. Redistribution subject to AIP license or copyright; see http://apl.aip.org/about/rights_and_permissions